Surface character in the experimental Fermi surface of epitaxial $ErSi_{1.7}$ (0001) by photoemission spectroscopy

J. A. Martín-Gago
Instituto Ciencia de Materiales de Madrid–CSIC, Campus de Cantoblanco, 28049 Madrid, Spain

J. Y. Veuillen
L.E.P.E.S.–C.N.R.S., Boîte Postale–116, 38046–Grenoble Cedex 9, France

C. Casado
Instituto Ciencia de Materiales de Madrid–CSIC, Campus de Cantoblanco, 28049 Madrid, Spain

T. A. Nguyen Tan
L.E.P.E.S.–C.N.R.S., Boîte Postale–116, 38046–Grenoble Cedex 9, France
(Received 28 May 1996; revised manuscript received 4 October 1996)

The electronic structure of erbium silicide, $ErSi_{1.7}$(0001), 100-Å-thick films epitaxially grown on Si(111), has been measured by angular-resolved ultraviolet photoemission (ARUPS) using synchrotron radiation. Valence-band spectra for different collection angles along the $\Gamma M\Gamma$ and ΓKM directions of the substrate Si(111)-(1×1) surface Brillouin zone (SBZ) and different Fermi-surface maps have been measured by the photoemission technique using photon energies of 21.2, 33, and 55 eV. The Fermi surface is characterized by hole and electron pockets at particular high-symmetry points in the SBZ. In opposition to what was expected considering both the crystallographic structure and calculated band structure, the shape of the Fermi-surface maps obtained for different photon energies are very similar. Moreover, the photoemission spectra using different photon energies show a very weak dispersion as a function of the **k** wave vector perpendicular to the surface ($\mathbf{k}_\perp$). All these findings suggest that the electronic states which contribute to the experimentally determined Fermi surface have a strong bidimensional character. No noticeable effect of the light polarization on the valence-band curves is observed indicating a hybrid nature of the involved orbitals. [S0163-1829(97)00804-7]

INTRODUCTION

Many studies have been devoted to the crystallographic and electronic structure of the erbium silicide films epitaxially grown on Si(111) surfaces. This interest is due to several reasons. Among them are the low Schottky barrier heights obtained with *n*-type silicon[1] and the very good crystalline quality of the epilayers.[2–4] $ErSi_{1.7}$ crystallizes in a defective AlB_2 structure. The bulk is built with a stacking of alternative hexagonal planes of Er and Si. In the Si planes, one out of six Si atoms is missing. These Si vacancies form a regular network and give rise to a $(\sqrt{3}\times\sqrt{3})R30°$ bulk structure ($R3$) (Refs. 4–6) in which recent surface x-ray-diffraction and medium-energy ion-scattering experiments have shown that Si atoms are displaced towards the vacancies and the Er atoms are displaced away from the vacancies.[6] The low-energy electron diffraction (LEED) pattern of the surface silicide also shows a $R3$ periodicity, which has been formally attributed to a periodic arrangement of the Si vacancies.[5] However, recent investigations by angle-resolved ultraviolet photoemission spectroscopy (ARUPS) combined with band-structure calculations,[7] atomic hydrogen adsorption,[8] and scanning tunneling microscopy[9,10] (STM) led to the conclusion that there are no vacancies at the surface and that the silicide is terminated in a buckled Si bilayer, where the upper Si atoms are relaxed forming a surface $R3$ superstructure.[10] The electronic structure of $ErSi_{1.7}$(0001) has been also extensively investigated both in the experimental and theoretical way.[11–15] The Si vacancies and the positions they occupy are found to greatly influence the electronic properties when compared to the one of the bulk silicide.[13] The ARUPS spectra given by the $ErSi_{1.7}$(0001) exhibits various structures, much more than transition-metal silicides. Some of these structures have been attributed to surface states.[11] It has been observed by ARUPS that the valence-band crosses the Fermi level at several points along the $\Gamma M\Gamma$ and ΓKM directions of the Si(111) surface Brillouin zone (SBZ). This observation has motivated the present work which aimed to investigated the electronic properties of the $ErSi_{1.7}$(0001) surface, in particular, its Fermi surface by means of the synchrotron radiation angle-resolved photoemission technique.

The Fermi surface is of great importance for understanding the properties of materials and epitaxial layers. The most common applied method to map a Fermi surface is the de Haas–van Alphen effect. Unfortunately, this technique requires high purity materials and in principle, low temperature, and then it is not suitable for measuring thin layers in ultrahigh vacuum (UHV) conditions. Recently, ARUPS appeared as a powerful tool for measuring Fermi surfaces in different compounds, layers, and specially electronic phase transitions.[16–18] The Fermi-surface shape is characteristic of the electronic dimensionality of a system.[19]

For a three-dimensional (3D) system the Fermi surface measured by ARUPS consists of continuous lines in the **k** space which correspond to slices related to the intersection between the 3D Fermi surface and the free-electron final-

state sphere.[17] However, for a 2D system, $\mathbf{k}_{\parallel}$ is conserved and there is no band dispersion along $\mathbf{k}_{\perp}$. Thus, the Fermi surface can be consider as a prismatic surface in the 3D $\mathbf{k}$ space. In 2D systems, the Fermi surface will appear to exhibit a shape which is independent of the photon energy. The unique appreciable difference when the photon energy varies is the size of the reciprocal space which is accessible (similar to a LEED pattern). Although $ErSi_{1.7}(0001)$ thick films have a 3D atomic structure, we have found strong experimental evidence to conclude that the electronic structure exhibits a 2D character. Particularly, the Fermi surface of the film is characterized by electron pockets at specific locations of the SBZ (M' points) and by a hole pocket of nearly circular shape centered around the surface Γ point. In addition, these electronic features do not depend on the photon energy as it does for a 2D system. All these findings support the idea that the photoemission technique is mainly sampling the surface and then, the experimentally measured Fermi surface is formed by 2D surface states.

EXPERIMENTAL DETAILS

100-Å-thick $ErSi_{1.7}(0001)$ films were prepared *in situ* by solid phase epitaxy on Si(111) substrates in UHV conditions. The crystalline quality of the films was controlled by LEED which showed the characteristic sharp $R3$ pattern of the $ErSi_{1.7}$ (0001) surface. More details about the preparation of $ErSi_{1.7}$ films can be found in Ref. 3.

Synchrotron-radiation photoemission experiments were performed on the PES-2 French-Spanish station in the beam line SU-6 at LURE laboratory (Orsay-France). Photons with energies ranging from 20 to 100 eV were available. The overall resolution (beam line plus analyzer) was better than 200 meV. The experimental station is also equipped with a x-ray tube, a He-I discharge lamp, and LEED optics for a sample characterization previous to the experiment. Spectra recorded at 21.2 eV of photon energy were measured using a discharge He-I UV lamp and a hemispherical analyzer with an energy resolution of around 100 meV. The angle of incidence of the photon beam in the photoemission spectra is defined with respect to the surface normal.

Fermi-surface measurements were performed by the method which consists of sequential data acquisition of the total photoemission intensity at the Fermi energy for a complete range of polar and azimuthal emission angles (θ,φ). The result is represented as a 2D pattern, where emission angles (θ,φ) are transformed in $\mathbf{k}_{\parallel}$ vectors and the photoemission intensity represented as an image (Fermi-surface map) in a gray scale (darker pixels correspond to lower intensities and brighter pixels to higher intensities). An electronic state approaching the Fermi edge will cause a net increase in the total number of emitted photoelectrons at the Fermi energy, and then, intensity maxima in the 2D maps indicate the points of the reciprocal space where a band crosses the Fermi edge. More details about the measurement procedure can be found in Ref. 17.

EXPERIMENTAL RESULTS

Figure 1 gathers a schematic extended zone representation of the first and second group of the SBZ of the $ErSi_{1.7}(0001)$ surface with respect to the main symmetry directions of the surface. The SBZ has been constructed taking into account the observed $R3$ LEED pattern. The $R3$ surface structure is marked in the figure as a continuous line and special points are labeled M' and K'. M' appears at 0.55 $Å^{-1}$ and the K' point appears at 0.63 $Å^{-1}$. In the following discussions a subscript index will label the symmetry points belonging to the second group of SBZ's, i.e., M_2', K_2', and Γ_2'. High-symmetry points M and K, of the bulk projected SBZ (dashed line) appear at 0.95 and 1.095 $Å^{-1}$, respectively. It is important to notice that the M point of the 1×1 structure also corresponds to the M' point for the second SBZ in the $R3$ superstructure and the K point in the 1×1 structure to the Γ_2' point in the second SBZ of the $R3$ superstructure. In order to calculate $\mathbf{k}_{\parallel}$ vectors, the standard free-electron final-state model was used and the work function has been chosen to be 4.7 eV (20).

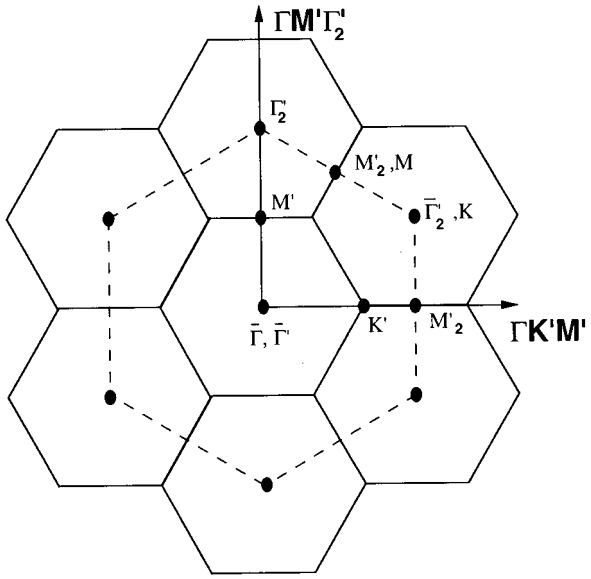

FIG. 1. Schematic representation of the first and second group of surface Brillouin zones (SBZ's) of the $(\sqrt{3}\times\sqrt{3})R30°$ structure (continuous line) and of the 1×1 structure (dashed line), indicating the high-symmetry points and directions. Points from the $(\sqrt{3}\times\sqrt{3})R30°$ are labeled as "'."

Figures 2(a)–2(c) represent different Fermi-surface maps recorded with photon energies of 21.2, 33, and 55 eV and recorded using the technique described in the experimental details section. Figure 2 gathers the total photoemission intensity in a narrow energy window which is centered at the Fermi edge of the silicide, recorded at different photon energies. Brighter zones on the pattern correspond to higher intensities at the Fermi edge and therefore to the presence of electronic states at the Fermi energy position. In the different figures the $R3$ SBZ has been drawn overimposed. Patterns have been recorded measuring a polar range of 60° and an azimuthal range of 120° and extrapolating the rest of the image taking advantage of the threefold symmetry of the system.

In the Fermi-surface map measured with a photon energy of 21.2 eV [Fig. 2(a)] the first SBZ is mainly seen. No information about higher SBZ's appearing at high $\mathbf{k}$, and then at high grazing emission angles, is accessible for this particular energy. In this pattern two different kinds of features can

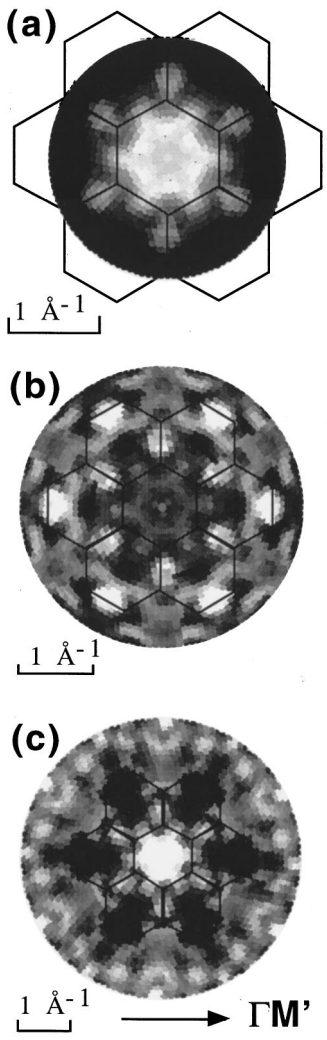

FIG. 2. Angular distribution of the photoemission intensity at the Fermi energy (Fermi-surface photoemission maps) for photon energies of 21 eV (a), 33 eV (b), and 55 eV (c). The first and second group of SBZ of the $(\sqrt{3}\times\sqrt{3})R30°$ superstructure has been drawn overimposed.

be observed. An enhancement of the intensity at points located very close to the M' points (see Fig. 1) and a nearly circular region centered in the Γ point with an approximate radius of $k_f \approx \frac{1}{2}|\Gamma K'| = 0.23$ Å^{-1}. The circular region seems to be distorted because it overlaps with the tail of the features appearing at the M' points.

Figure 2(b) represents a Fermi-surface pattern recorded with a photon energy of 33 eV. In this figure the enhancement of the emission at the M' points are clearly seen, especially those of the second SBZ. Albeit with difficulty, the inner circle is observed. Differences in intensity between equivalent features for different energies and angles could be assigned to the different cross-section and polarization effects for this particular $\mathbf{k}$ point (θ,φ). Particularly, some contours in the Fermi-surface maps are not symmetric around the critical point [e.g., M_2' points in Fig. 2(b)]. The photoemission intensity depends strongly on the angle between the light polarization vector and the electronic orbital momentum of the emitted photoelectron[20] (i.e., the polar angle, θ) and thus, the symmetry of the contours is exclusively conserved in azimuthal scans (i.e., circularly around the photoemission map). Figure 2(c) has been measured using photons with an energy of 55 eV. At this photon energy most of the second group of SBZ's appear in the pattern. Again, both kinds of features (enhancement of intensity in M' points and circle around the Γ point), already observed in Figs. 2(a) and 2(b), are clearly seen. Thus, it could be stated that the same electronic features appear in the Fermi-surface maps for different photon energies.

A film of more than 100 Å thick can be considered as a 3D compound. Thus, when the photon energy varies, different cuts on the 3D Fermi surface are expected and lead to patterns which are made of figures (lines) showing different symmetries. However, in 2D compounds the electronic structure as seen by the photoemission process, should not be dependent on the photon energy. Thus the same kind of features are displaced for all energies. The only difference appears in the size of the SBZ as observed in Fig. 2. In this figure it is also clear that the experimental Fermi-surface exhibits the same shape whatever the photon energy.

To know whether the enhancement of intensity in the 2D maps corresponds either to a band crossing the Fermi edge or to a state which approaches close to the Fermi energy, and to determine with more precision the $\mathbf{k}_f$ value, ARUPS valence-band spectra along the directions where a maximum of intensity is seen in the Fermi-surface map have been measured. Figure 3 represents a series of curves taken with a photon energy of 21.2 eV along the $\Gamma M'\Gamma_2'$ [Figs. 3(a) and 3(b)] and along the $\Gamma K' M_2'$ directions [Figs. 3(c) and 3(d)]. The value of the $\mathbf{k}_\parallel$ in Å^{-1} at the Fermi energy position is indicated for each spectrum. In this figure, the electronic states which are the closest to the Fermi energy are clearly resolved in energy regions centered around the points which belong to the Fermi surface. In Figs. 3(a) and 3(c) the peaks are seen to move towards the Fermi edge if the $\mathbf{k}$ value moves away from the M' points, whereas in Figs. 3(b) and 3(c) the peaks move away from the Fermi energy when the k value moves away from the Γ point. Along the $\Gamma K' M_2'$ direction [Fig. 3(c)], the intersection occurs at around 0.70 and 1.20 Å^{-1}, which correspond to an approximate k distance from the M_2' point of 0.25 Å^{-1}. Along the $\Gamma M'\Gamma_2'$ direction [Fig. 3(a)] the same behavior is observed but the distance in the $\mathbf{k}$ space from the M' points to the crossing points is slightly smaller: around 0.10 Å^{-1}. This kind of upward band dispersion from a critical point is called electron pocket. From now on, the $\mathbf{k}$ position where the band crosses the Fermi edge from a M' point will be referred as $\mathbf{k}_{\rm fe}$. It is important to note that the $\mathbf{k}_{\rm fe}$ is higher along the $\Gamma K' M_2'$ direction than along $\Gamma M'\Gamma_2'$. This asymmetry is also appreciated in maps in Fig. 2 as an elongation of the points. The existence of this state which crosses over the Fermi energy in the region of the reciprocal space close to the M' points induces the enhancement of intensity (clearer spots) measured in the Fermi-surface maps of Fig. 2. Moreover, in Figs. 3(b) and 3(c) is shown the existence of a hole pocket, i.e., electronic states approaching the Fermi energy when $\mathbf{k}$ moves towards the Γ point. The crossing point will be labeled as $\mathbf{k}_{\rm fh}$.

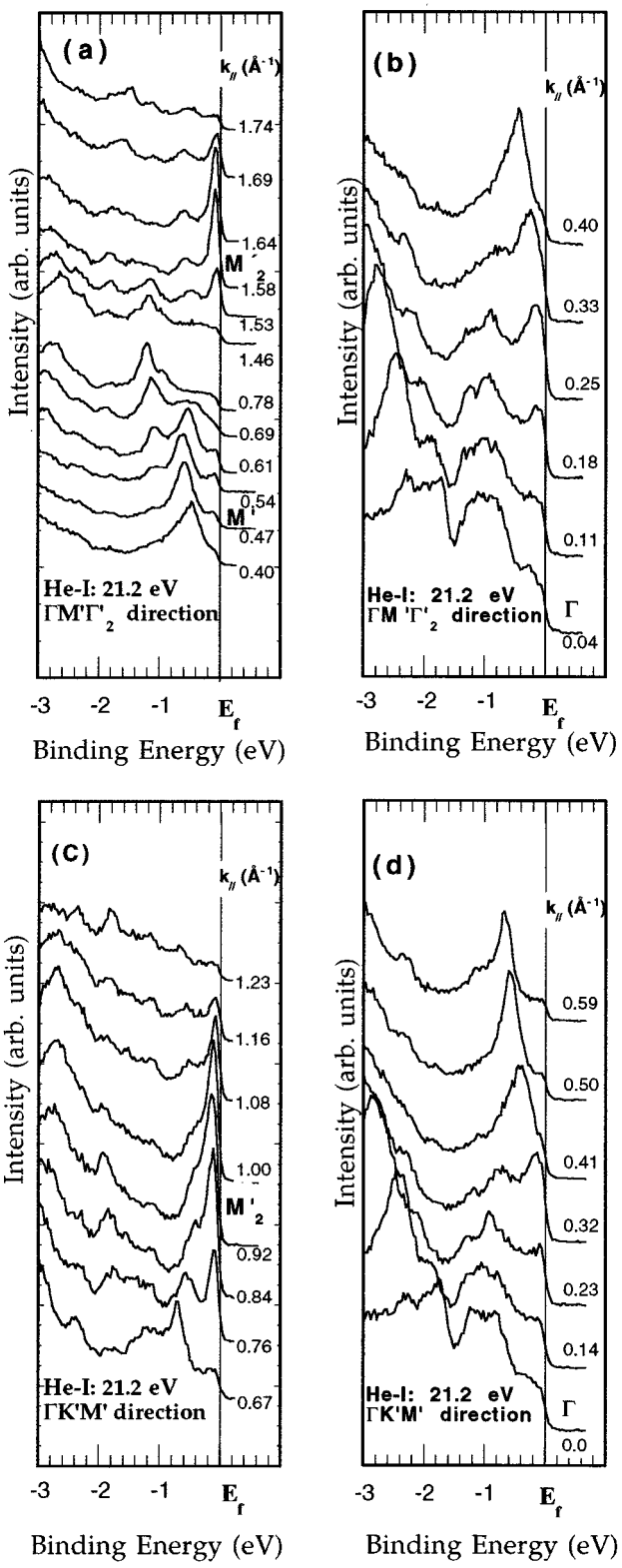

FIG. 3. Angular-dependent photoemission spectra along the high-symmetry directions of the SBZ. The photon energy is 21.2 eV from He-I radiation. The value of $\mathbf{k}_{\|}$ at the Fermi energy is displayed at the beginning of each spectrum. (a) and (b) have been recorded along $\Gamma M' \Gamma_2'$ and (c) and (d) along the $\Gamma K' M_2'$ direction.

To determine more accurately the position where the bands cross the Fermi edge, a band dispersion for the energy region close to the Fermi energy has been plotted in Fig. 4 using, among others, the ARUPS curves of Fig. 3. Due to the

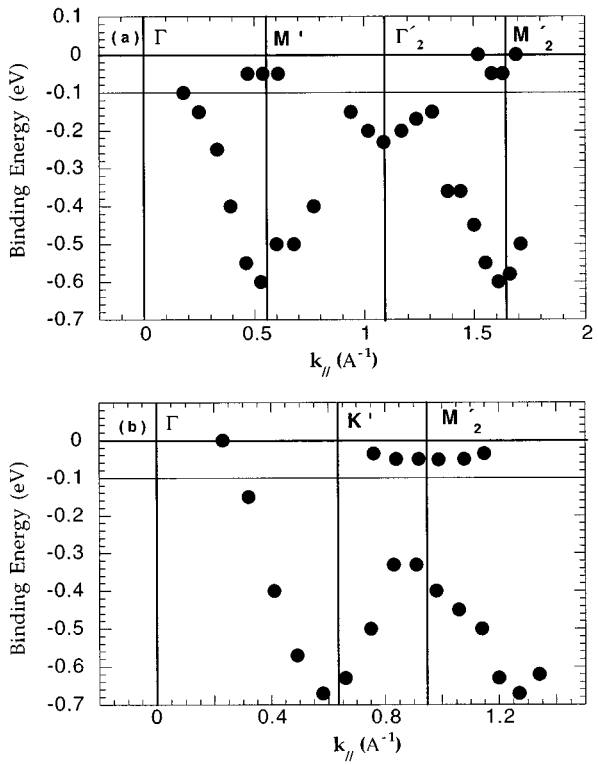

FIG. 4. Band dispersion along $\Gamma M' \Gamma_2'$ (a) and along $\Gamma K' M_2'$ (b) directions. Electronic states with binding energies above the hairline (at -0.1 eV) will contribute to the intensity of the Fermi-surface maps.

natural width of the valence-band electronic states[20] and to the experimental energy resolution, the peaks appearing with binding energies smaller than 0.1 eV will contribute to the intensity of the Fermi-surface maps.[18] Thus, the experimental points of Fig. 4 above the hairline can be considered as belonging to the Fermi surface. This figure clearly shows the crossing points described above, which corresponds to electron pockets centered around the M' points of the SBZ of the $ErSi_{1.7}$. In addition to that, a band showing a downwards dispersion when one moves away from the Γ point is seen in both directions. These bands form a hole pocket of around 0.20 $Å^{-1}$ centered around the Γ point. This feature generates the nearly circular shape bright region at the inner part of the SBZ which is observed in Fig. 2(a).

For clarity, Fig. 5 contains a sketch of the previously described 2D Fermi surface from the photoemission point of view. In this scheme, hole and electron pockets are indicated. It can be concluded that the Fermi surface consists of small and asymmetric electron pockets around the M' points, with an average $\mathbf{k}_{fe}=0.18$ $Å^{-1}$ and a hole pocket centered on the Γ point with an average $\mathbf{k}_{fh}=0.20$ $Å^{-1}$.

Figure 6 represents a series of photoemission spectra recorded for different photon energies at normal emission and in sp-polarization conditions (incidence angle of 45°). For these conditions, $\mathbf{k}_{\|}=\mathbf{0}$ and one is sampling $\mathbf{k}_{\perp}$ when the photon energy is varied.[20] In these curves two energy regions can be seen. The region near the Fermi energy ($E_b<1.5$ eV, labeled as I) and the region further apart from it ($E_b>1.5$ eV, labeled as II). Region I is characterized by two electronic

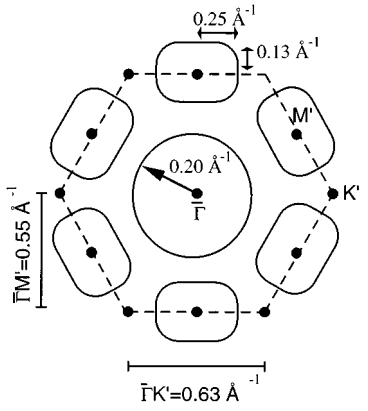

FIG. 5. Schematic representation of the Fermi surface characterized by asymmetric electron pockets around M' points and a nearly circular hole pocket around the surface Γ point. Critical points of the $(\sqrt{3}\times\sqrt{3})R30°$ SBZ are indicated in the figure.

states, one at -0.2 eV and the other at -0.93 eV. These states show only a weak dispersion (<0.2 eV). The state which is the closest to the Fermi edge is clearly resolved in spectra recorded with photon energies higher than 28 eV. Its binding energy is constant and equals -0.2 eV. The fact that the state is not visible with photon energies smaller than 25 eV should be attributed to a low cross section for these particular energies rather than to a crossing over the Fermi energy, which is seen as a continuous approach of the state towards the Fermi edge. The total difference between $\mathbf{k}_\perp$ vectors of the states in the region I is around 1.5 Å^{-1}. For the $ErSi_{1.7}$, $c^*=1.54$ Å^{-1}, thus a complete BZ was covered in the spectra of Fig. 6 and therefore, different features should not appear for other different photon energies. These data are similar to the ones reported for the Gd silicide surface.[21]

The region labeled as II exhibits very wide and dispersive electronic states suggesting a $\mathbf{k}_\perp$ broadening mechanism which could be induced by a short mean free path of the photoelectrons.[22] Short mean free paths, in the order of the interplane distance, can lead to an important weighting of the surface features with respect to the bulk ones in the photoemission signal and to a broadening of the bulk structures. This fact would then contribute to the enhancement of the surface contribution to the photoemission spectra relative to the bulk ones.

Figure 7(a) shows different photoemission spectra recorded at the M_2' point for different photon energies and polarization conditions (s and p polarization and unpolarized radiation). The incidence angle of the radiation with respect to the surface normal for the different spectra are indicated in the figure. It is important to notice that in the energy range close to the Fermi edge (I) all spectra show similar shapes. The invariance with the photon energy of the valence band at the critical points of the SBZ suggests, again, a bidimensional character of the electronic states. Figure 7(b) represents a normal-emission spectra for p and sp polarization. Both spectra are very similar. The low polarization dependence of the normal-emission spectra [Fig. 7(b)] and of the M_2' point spectra [Fig. 7(a)] indicates that the electronic states in region I have a hybrid Er $5d$ and Si $3p$ character as it has been previously claimed in band-structure calculations.[7] The invariance of spectra for different energies is also observed in the Γ_2' point (data not shown, see, e.g., Ref. 11).

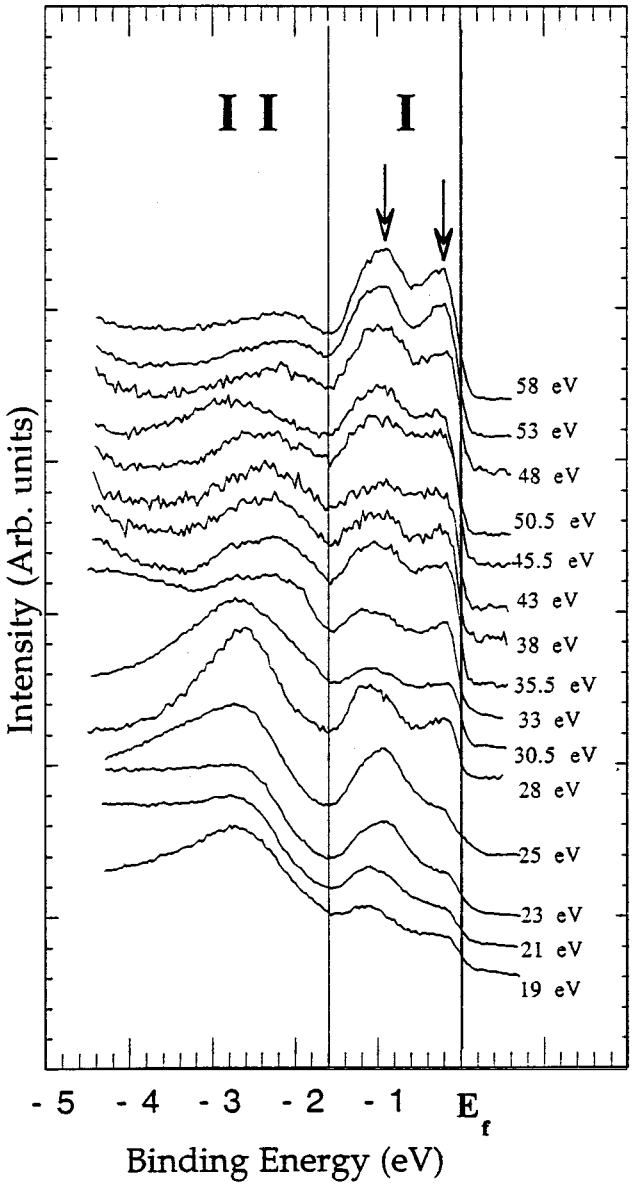

FIG. 6. Variable photon energy photoemission spectra recorded at normal emission. The angle of incidence of the radiation was 45° (sp polarization).

DISCUSSION

The bidimensional character suggested by the photoemission experiments seems a peculiar result. Different to what is observed in other laminar compounds, as graphite which has highly inert planes separated by 3.35 Å and weakly bonded between them, the $ErSi_{1.7}$ presents a short distance between planes ($c/2=2.045$ Å) and a metallic bonding between the different planes. In addition to that, a film thickness of 100 Å corresponds to more than 25 atomic cells in the direction perpendicular to the surface, and thus a 3D behavior in UV photoemission can be anticipated.[20] For this reason, the elec-

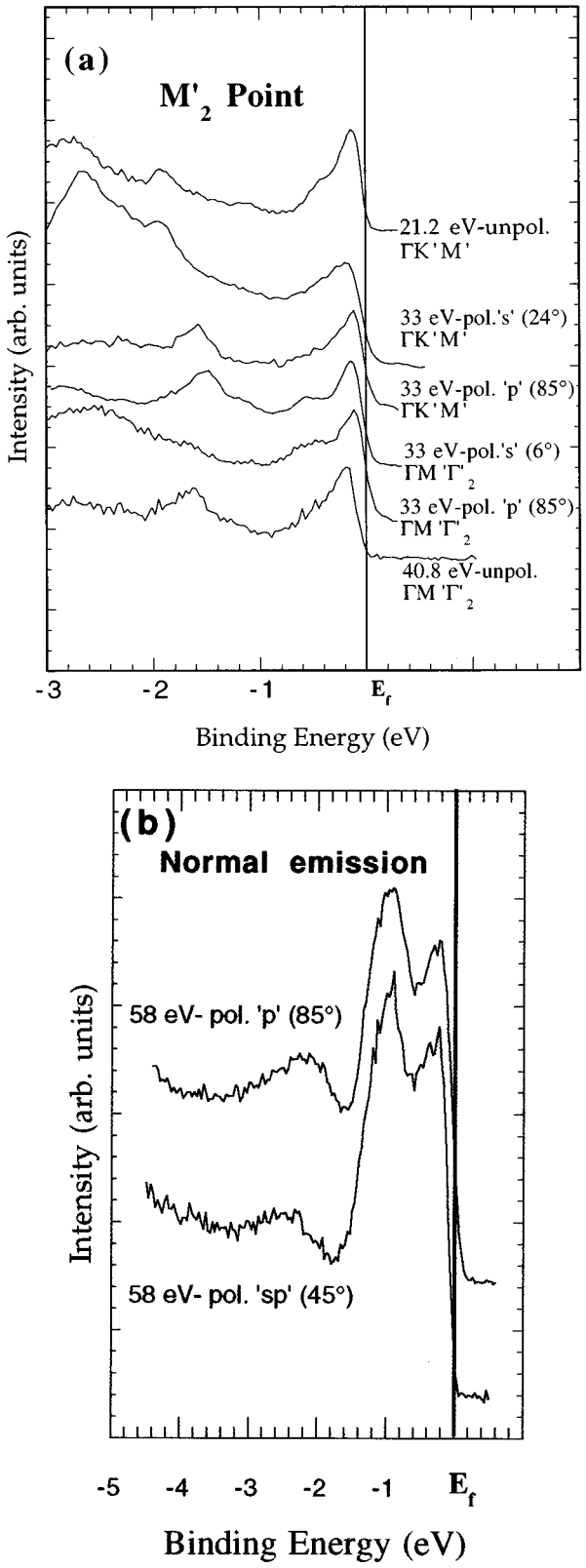

FIG. 7. (a) Photoemission spectra recorded at the M_2' point of the SBZ for different light polarizations and photon energies. (b) Photoemission spectra recorded in normal emission for ''*sp*'' polarization (angle of incidence of 45°) and ''*p*'' polarization (angle of incidence of 85° with respect to the surface normal).

tronic structure is not expected to have a 2D character as it occurs for the 1-ML-thick silicide.[25] Furthermore, band-structure calculations have predicted the existence of a 3D Fermi surface.

Previously reported calculated band structures in the ΓA direction, i.e., perpendicular to the surface[14] show a group of three flat bands with around -0.4 eV binding energy and another group of twofold degenerated bands which disperse from -1.0 to -1.5 eV when the $\mathbf{k}_\perp$ moves from Γ to A in reciprocal space. The first group has been associated to Er $5d$ states and one of the bands crosses the Fermi edge at $\mathbf{k}_\perp \approx 1/2\ |\Gamma A| = 0.4$ Å^{-1}, which leads to a 3D Fermi surface. In our experimental data (Fig. 6), there is not a signature for the presence of this later band and only the flat and nondispersive bands are found. The other group of bands has been associated to the presence of Si vacancies in the bulk and then arise from bonding interactions between Si σp states and Er d states. They could correspond in the experimental data (Fig. 6) to the states which are seen at -0.9 eV. However the fact that these structures are visible even for p polarization (Fig. 7) suggests that they are derived from states with an important component which is perpendicular to the surface normal. Moreover, previous studies of H adsorption suggest that they are surface states.[8] This can be the reason why it is nondispersive with the photon energy.

The disagreement between the band-structure calculations and the photoemission results (present and previously reported by other groups)[12,14] could be due to the fact that the calculations reflect the bulk electronic structure of the silicide. On the other hand, a very short value of the mean free path for these kinetic energies is likely. This could be responsible for the fact that the photoemission technique mainly probes the surface features of the electronic structure which cannot be readily compared to bulk band-structure calculations.

Another argument supporting the observed 2D character in the measured Fermi surface on the $ErSi_{1.7}$ films is the close relationship with the Fermi surface of a 2D erbium silicide 1 ML thick in epitaxially grown Si(111). By LEED, ARUPS, and STM it has been clearly demonstrated that this silicide consists of a continuous layer of 1 ML thick, spreading over the Si(111) surface.[23,24] Also it has been shown that the SBZ presents a (1×1) symmetry and a Fermi surface which is characterized by a hole pocket with a $\mathbf{k}_{\mathrm{fh}}=0.16$ Å^{-1} centered around the Γ point and electron pockets of $\mathbf{k}_{\mathrm{fe}}=0.1$ Å^{-1} centered around the M points of the 1×1.[25] As schematically represented in Fig. 5 the Fermi surface of the $ErSi_{1.7}$ can be reproduced by backfolding the one of the 2D erbium silicide (see Fig. 8 of Ref. 7) in order to transform the 1×1 symmetry into the $R3$ symmetry.

SUMMARY

The electronic structure of the epitaxial $ErSi_{1.7}$ films on Si(111) presents a bidimensional character from the angular-resolved and variable photon energy photoemission point of view. The experimentally determined Fermi surface consists of asymmetrical electron pockets at the M' points of the SBZ and a hole pocket centered around the Γ point of the SBZ. This surprising 2D character could originate from a

mean free path of the photoelectrons which should be in the order of the interplanar distance in erbium silicide. No noticeable effect of the light polarization on the valence-band curves is observed, indicating a hybrid nature of the involved orbitals.

ACKNOWLEDGMENTS

This research is in the frame of the Spanish CICYT project No. PB94-0053. One of us (J.A.M.-G.) is grateful to the bilateral cooperation program CNRS-CSIC.

[1] M. H. Unewiseand and J. W. Storey, J. Appl. Phys. **72**, 2367 (1992).
[2] F. Arnaud d'Avitaya, A. Peris, J. C. Obelin, Y. Campidelli, and J. A. Chroboczek, J. Appl. Phys. **54**, 2198 (1989).
[3] D. B. B. Lollman, T. A. Nguyen Tan, J. Y. Veuillen, P. Muret, M. Brunel, and J. C. Dupuy, Appl. Surf. Sci. **65/66**, 704 (1993).
[4] F. H. Kaatz, J. Van der Spiegel, and W. R. Grahan, in *Epitaxial Heterostructures*, edited by D. W. Shaw, J. C. Bean, V. G. Keramidas, and P. S. Peercy, MRS Symposia Proceedings No. 198 (Materials Research Society, Pittsburgh, 1990), p. 601.
[5] R. Baptist, S. Ferrer, G. Grenet, and C. H. Poon, Phys. Rev. Lett. **64**, 311 (1990).
[6] M. Lohmeier, W. J. Huisman, E. Vlieg, A. Nishiyama, C. L. Nicklin, and T. S. Turner, Surf. Sci. **345**, 247 (1996).
[7] P. Wetzel, S. Saintenoy, C. Pirri, D. Bolmont, and G. Gewinner, Phys. Rev. B **50**, 10 886 (1994).
[8] J. Y. Veuillen, T. A. Nguyen Tan, S. Ladas, and S. Kennou, Phys. Rev. B **52**, 10 796 (1995).
[9] T. P. Roge, F. Palmino, C. Savall, J. C. Labrenne, P. Wetzel, C. Pirri, and G. Gewinner, Phys. Rev. B **51**, 10 998 (1995).
[10] J. A. Martin-Gago, J. M. Gomez-Rodriguez, and J. Y. Veuillen, following paper, Phys. Rev. B **55**, 5136 (1997).
[11] J. Y. Veuillen, L. Magaud, D. B. B. Lollman, and T. A. Nguyen Tan, Surf. Sci. **269/270**, 964 (1992).
[12] G. Allan, I. Lefebre, and N. E. Christensen, Phys. Rev. B **48**, 8572 (1993).
[13] L. Magaud, J. Y. Veuillen, D. B. B. Lollman, T. A. Nguyen Tan, D. A. Papapconstantoupoulos, and M. J. Mehl, Phys. Rev. B **46**, 1299 (1992).
[14] L. Stauffer, C. Pirri, P. Wetzel, A. Mharchi, P. Paki, D. Bolmont, G. Gewinner, and C. Minot, Phys. Rev. B **46**, 13 201 (1992).
[15] L. Stauffer, A. Mharchi, S. Saintenoy, C. Pirri, P. Wetzel, D. Bolmont, and G. Gewinner, Phys. Rev. B **52**, 11 932 (1995).
[16] P. Aebi, J. Osterwalder, P. Schawaller, L. Schlapbach, M. Shimoda, T. Mochiku, and K. Kadowaki, Phys. Rev. Lett. **72**, 2757 (1994).
[17] P. Aebi, J. Osterwalder, R. Fasel, D. Naumovic, and L. Schlapbach, Surf. Sci. **307–309**, 917 (1994).
[18] K. E. Smith and S. D. Kevan, Phys. Rev. B **43**, 3986 (1991).
[19] K. E. Smith, K. Breuer, M. Greenblatt, and W. McCarrol, Phys. Rev. Lett. **70**, 3772 (1993).
[20] F. J. Himpsel, Appl. Opt. **19**, 3964 (1980), and references therein.
[21] W.A. Henle, M. G. Ramsey, F. P. Metzer, R. Cimino, and W. Braun, Solid State Commun. **71**, 657 (1989).
[22] F. J. Himpsel and B. Reihl, Phys. Rev. B **28**, 574 (1983).
[23] P. Wetzel, C. Pirri, P. Paki, D. Bolmont, and G. Gewinner, Phys. Rev. B **47**, 3677 (1993).
[24] J. A. Martin-Gago, J. M. Gomez-Rodriguez, and J. Y. Veuillen, Surf. Sci. **366**, 491 (1996).
[25] P. Wetzel, C. Pirri, P. Paki, P. Peruchetti, D. Bolmont, and G. Gewinner, Solid State Commun. **82**, 225 (1992).